PILES

LATERAL DYNAMIC RESPONSE OF CONSTRAINED-HEAD PILES

By Alvaro Velez,[1] George Gazetas,[2] M. ASCE, and Raman Krishnan[3]

ABSTRACT: This paper utilizes an efficient finite-element formulation to study the dynamic response characteristics of single constrained-head piles embedded in a soil stratum whose modulus is proportional to depth from the surface. The excitation consists of a harmonic horizontal force or moment applied at the pile head, and the soil is modeled as a linear hysteretic medium. The results of a comprehensive parametric study are presented in the form of non-dimensional graphs from which one can readily estimate static and dynamic stiffnesses and effective damping ratios of piles in many practical situations. For flexible piles, in particular, simple, yet sufficiently accurate, algebraic formulas are derived, valid for a wide range of problem parameters. Finally, the concept of an effective soil modulus is introduced to elucidate the importance of soil nonhomogeneity and to gain valuable insight to the mechanics of the problem.

INTRODUCTION

The dynamic behavior of end-bearing and floating single piles subjected to horizontal and moment loading has been studied extensively in recent years. The developed formulations may be broadly classified into three categories: (1) Dynamic Winkler-foundation type formulations, which neglect the dynamic coupling between forces and displacements at various points along the pile-soil interface (6,11,15,18,19); (2) analytical continuum type formulations which express the lateral dynamic soil pressure, in terms of the natural modal displacements of the soil deposit in vertical shear waves (9,12,17,30); and (3) dynamic finite-element formulations which use axisymmetric elements and special "energy-transmitting" boundaries (1,4,14).

With these formulations parametric studies have been conducted and solutions are now available for a variety of idealized situations (4,6,9,11,12,14,15,17,19,27,31). However, most of the presented results apply to homogeneous soil masses. Although for deep uniform deposits of stiff clays the assumption of ideal homogeneous soil may be a satisfactory approximation, consideration of nonhomogeneity would be more realistic in many practical situations, since soil stiffness usually increases with depth. Unfortunately, the practicing geotechnical engineer involved in preliminary design of piles against dynamic loading has little choice (before embarking into detailed analyses using available computer codes) other than to use available homogeneous solutions with an appropriately selected "effective" modulus for the soil. Yet, there is very

[1]Grad. Student, Dept. of Civ. Engrg., Rensselaer Polytechnic Inst., Troy, N.Y. 12181.

[2]Assoc. Prof., Dept. of Civ. Engrg., Rensselaer Polytechnic Inst., Troy, N.Y. 12181.

[3]Grad. Student, Dept. of Civ. Engrg., Rensselaer Polytechnic Inst., Troy, N.Y. 12181.

Note.—Discussion open until January 1, 1984. To extend the closing date one month, a written request must be filed with the ASCE Manager of Technical and Professional Publications. The manuscript for this paper was submitted for review and possible publication on August 30, 1982. This paper is part of the Journal of Geotechnical Engineering, Vol. 109, No. 8, August, 1983. ©ASCE, ISSN 0733-9410/83/0008-1063/$01.00. Paper No. 18166.

little published information to guide the selection of such a modulus, and the engineer has to rely upon his own, often limited, experience.

The major goal of this paper is to present solutions which may be readily utilized in practice to obtain realistic estimates of dynamic lateral deformations of piles embedded in nonhomogeneous soil profiles. To this end, the results of a comprehensive parametric study are presented in the form of nondimensional graphs and simple expressions, valid for a wide range of the crucial problem parameters. The results have been obtained for a soil stratum having a linearly increasing stiffness with depth—an idealization adopted not only for its simplicity but, also, for its special ability to represent actual soil behavior under lateral pile loading, as explained later in the paper. Therefore, the presented solutions will be useful even for soil profiles where a less rapid increase of modulus with depth seems appropriate.

A second objective of the paper is to focus on the effects of soil nonhomogeneity on the lateral static and dynamic response of piles. By trying to physically explain these effects, valuable insight is gained into the mechanics of the problem. It is, moreover, shown that the choice of an "effective" soil modulus depends not only on the type of loading (force or moment) but, also, on its frequency of oscillation. Finally, criteria are developed to define when a pile is 'flexible' under static and dynamic loads. It is worth emphasizing that even some of the *static* results presented in this paper are mostly new in the geotechnical literature.

Statement of the Problem and the Nonhomogeneous Soil Model

Figure 1 sketches the system to be studied. A constrained-head circular pile of diameter d and length L is embedded in a nonhomogeneous soil stratum underlain by rigid bedrock at depth L. The pile is treated as a linear elastic beam having constant Young's modulus, E_p, and mass density, ρ_p. The soil is assumed to be a linear hysteretic medium with a constant Poisson's ratio, ν, a constant mass density, ρ_s, and a Young's modulus increasing linearly with depth

$$E(z) = E_s \frac{z}{d} \qquad (1)$$

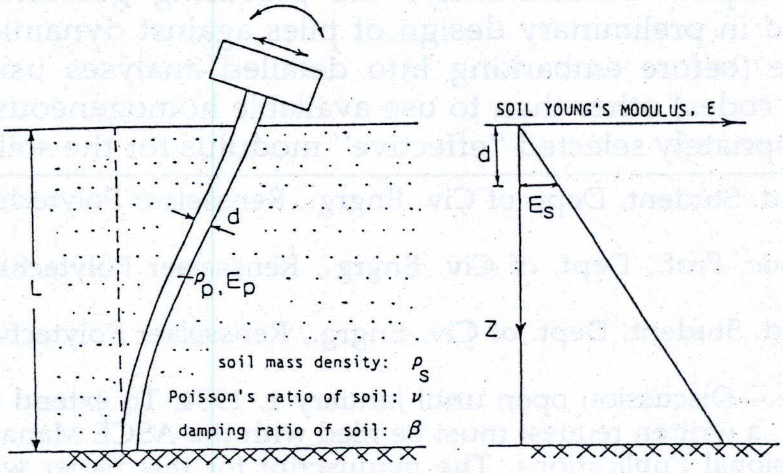

FIG. 1.—End-Bearing Constrained-Head Pile in Soil Stratum with Modulus Proportional to Depth

in which E_s = the modulus at a depth $z = d$. The internal energy dissipating characteristics of the soil are described through a frequency-independent hysteretic damping ratio, $\beta(z)$, decreasing function of depth, as explained later.

The constraint at the pile head may arise from the presence of a pile-cap or of a foundation mat; also, in some structures such as off-shore platforms, an elastic constraint may be provided through a direct connection of the pile with the superstructure. In all cases, the dynamic response of the foundation to an arbitrary harmonic excitation may be easily computed once the dynamic stiffnesses (also called dynamic impedances) at the top of the pile are known for each particular frequency of interest. With lateral loading, three impedances must be specified, $\mathcal{K}_{HH}$, $\mathcal{K}_{MM}$ and $\mathcal{K}_{HM}$, associated with swaying, rocking and coupled swaying-rocking oscillations, respectively. For each particular sinusoidal excitation (force or moment) having frequency ω, a dynamic impedance is defined as the ratio between the magnitudes of excitation and of the resulting steady-state displacement or rotation at the pile head. For example, the swaying impedance is defined as

$$\mathcal{K}_{HH} = \frac{P_o \exp(i\omega t)}{u_o \exp[i(\omega t + \phi)]} \quad \ldots\ldots (2)$$

in which $P = P_o \exp(i\omega t)$ = the horizontal dynamic force and $u = u_o \exp[i(\omega t + \phi)]$ = the resulting steady-state horizontal displacement when no rotation is allowed at the pile top ('fixed-head' pile). Figure 2 illustrates the definitions of the three impedances. The phase-angle difference, ϕ, between dynamic displacement and excitation is due to the presence of damping in the system; part of the input energy is dissipated through hysteretic action in the soil (internal damping), while another part gets lost with waves spreading outward away from the pile (radiation damping). It has become traditional in the soil dynamics literature (e.g., 1, 6, 8, 11, 14, 17, 26) to use complex notation and express the dynamic impedances in the form, e.g.,

$$\mathcal{K}_{HH} = K_{HH} + i\omega C_{HH} \quad \ldots\ldots (3)$$

in which $i = \sqrt{(-1)}$. The real component of the impedance, K_{HH}, may

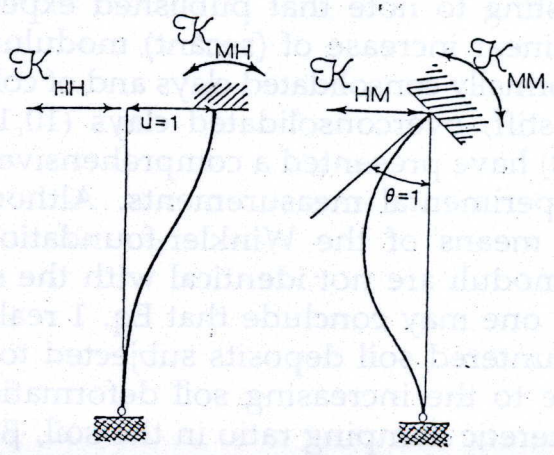

FIG. 2.—Definition of Three Pile-Head Impedances

be interpreted as a 'spring' stiffness while C_{HH} can be thought of as a 'dashpot' coefficient. The word "constant" has been avoided because both K_{HH} and C_{HH} are functions of frequency. It is convenient to introduce a dimensionless coefficient, D_{HH}, in place of C_{HH} (dimension $[FTL^{-1}]$); the two coefficients are related by

$$D_{HH} = \frac{C_{HH}}{2\frac{K_{HH}}{\omega}} \qquad (4)$$

D_{HH} can be considered to be the effective critical damping ratio in the system (1,6). A frequency-independent D_{HH} represents hysteretic damping, associated with material nonlinearities, while D_{HH} increasing with frequency represents viscous damping, arising from the loss of energy due to outward spreading waves.

At this point some comments seem appropriate concerning the selection of a nonhomogeneous soil model characterized by moduli increasing linearly with depth. Clearly, the simplicity of the model has been a factor in our consideration. More important, however, is the fact that this model appears capable of representing with reasonable accuracy many actual soil profiles. For instance, in normally consolidated clays, the undrained Young's modulus, E_u, is in many cases proportional to the undrained shear strength; the latter is linearly related to the effective mean confining pressure which, in turn, is proportional to depth. Thus, E_u is proportional to depth (i.e., of the form of Eq. 1).

Furthermore, an additional argument may be advanced in favor of the chosen model when considering lateral loading of the soil by a pile. That is, a linear analysis with soil stiffness being proportional to depth may indirectly take into account soil nonlinearity, as values of the soil secant modulus near the surface are likely to be reduced because of the developing large shear strains associated with the large pile deflections near the pile head. In other words, even when the profile of soil moduli determined at very low shear strain amplitudes ($\gamma \leq 10^{-6}$) exhibits a milder than the linear increase with depth, as e.g., in case of sand and overconsolidated-clay deposits, the actual profile of secant moduli consistent with the expected levels of strain may still be better approximated with the chosen linear variation (Eq. 1).

It is interesting to note that published experimental results strongly support the linear increase of (secant) modulus with depth not only in deposits of normally consolidated clays and of cohesionless soils (10,24,29), but even in stiff, overconsolidated clays (10,16,25). Jamiolkowski and Garassino (10) have presented a comprehensive list of the results of such published experimental measurements. Although these tests were interpreted by means of the Winkler-foundation model and, thus, the backfigured moduli are not identical with the soil Young's moduli considered here, one may conclude that Eq. 1 realistically represents many actually encountered soil deposits subjected to lateral pile loading.

In response to the increasing soil deformation near the ground surface, the hysteretic damping ratio in the soil, $\beta(z)$, is taken as a decreasing function of depth; in this study, it varies from a maximum value of 8% immediately below the surface to a minimum of 2% at greater depths.

Sensitivity studies, documented by the writers (31), have shown that the exact distribution of damping at intermediate depths has no substantial effect on pile response, as long as the average value of β over the 'active' pile length remains the same. Hence, only this average value, β, is reported in the sequel.

Results of Finite Element Parameter Study

The finite-element formulation of Blaney, Kausel and Roesset (4) has been used in this study. The geometry is idealized by a cylindrical region surrounding the pile and a "far-field" of semi-infinite horizontal extent. The pile is modeled as a series of beam elements and it is assumed to be hinged at the baserock (i.e., at $z = L$). Key ingredient of the formulation is the derivation of a so-called "consistent boundary" matrix which is placed at the edge of the central cylindrical region and reproduces the effect of the "far field" in a rigorous fashion (13). Thus, a theoretically perfect absorption of outward spreading waves is accomplished and no artificial trapping of wave energy can occur. Moreover, in cases where the soil properties do not change in the horizontal direction, as in the present study, the "consistent boundary" can be placed directly at the pile-soil interface. Hence, a substantial economy is achieved and it becomes quite feasible to conduct comprehensive parameter studies, like the one reported herein and those in Refs. 1, 4 and 6. For more details see the aforementioned original publications.

Results are presented for each of the three impedances, expressed in terms of the normalized stiffnesses

$$\frac{K_{HH}}{(d\,E_s)};\quad \frac{K_{MM}}{(d^3E_s)};\quad \text{and}\quad \frac{K_{HM}}{(d^2E_s)} \qquad (5)$$

and the corresponding effective damping ratios, D_{HH}, D_{MM} and D_{HM}. The above six quantities depend on the following dimensionless parameters of the system: (1) The ratio E_p/E_s of the Young's modulus of the pile over the Young's modulus of the soil at depth $z = d$ (Eq. 1); (2) the slenderness ratio, L/d; (3) the dimensionless frequency factor, $a_s = \omega d/V_s$, in which V_s = the S-wave velocity of the soil at $z = d$; (4) the internal hysteretic damping ratio in the soil, β, assumed to be either a constant or a decreasing function of depth; (5) the Poisson's ratio, ν, of the soil; and (6) the ratio of mass densities, ρ_p/ρ_s, of pile and soil.

The presented non-dimensional plots, derived herein for circular piles of solid, uniform cross-section with diameter d, can also be used for piles with other cross-section shapes. To this end, an equivalent diameter, d', and an equivalent Young's modulus, E_p', must be first defined. d' is taken as the width of the pile measured perpendicular to the direction of loading; E_p' is selected so that the product $E_p'\,\pi(d')^4/64$ is the same as E_pI_p of the actual pile. For example, for a pipe pile of modulus E_p, external diameter d_o and internal diameter d_i, the equivalent solid pile has: $d' = d_o$ and $E_p' = E_p(d_o^4 - d_i^4)/d_o^4$. The equivalence is mathematically exact in this case (pipe pile), but it is only an approximation for other shapes, such as with square or H-piles.

By choosing Young's modulus to normalize the stiffnesses (Eq. 5) and

TABLE 1.—Cases Studied

E_p/E_s (1)	L/d (2)	l_s/d (3)	Nature of static behavior (4)	l_d/d (5)	Nature of dynamic behavior (6)
58	5	4.1	'Flexible'	8.2	Non-'Flexible'
	10		'Flexible'		'Flexible'
	15		'Flexible'		'Flexible'
	25		'Flexible'		'Flexible'
	40		'Flexible'		'Flexible'
290	5	5.6	Almost 'Flexible'	10.1	Non-'Flexible'
	10		'Flexible'		Almost 'Flexible'
	15		'Flexible'		'Flexible'
	25		'Flexible'		'Flexible'
	40		'Flexible'		'Flexible'
1,450	5	8.0	Non-'Flexible'	12.5	Non-'Flexible'
	10		'Flexible'		Non-'Flexible'
	15		'Flexible'		'Flexible'
	25		'Flexible'		'Flexible'
	40		'Flexible'		'Flexible'
29,000	5	14.9	Non-'Flexible'	19.8	Non-'Flexible'
	10		Non-'Flexible'		Non-'Flexible'
	15		'Flexible'		Non-'Flexible'
	25		'Flexible'		'Flexible'
	40		'Flexible'		'Flexible'
145,000	5	20.5	Non-'Flexible'	24.6	Non-'Flexible'
	10		Non-'Flexible'		Non-'Flexible'
	15		Non-'Flexible'		Non-'Flexible'
	25		'Flexible'		Almost 'Flexible'
	40		'Flexible'		'Flexible'

to represent the contrast in stiffness between pile and soil (E_p/E_s), the effect of ν and ρ_p/ρ_s was found to be minimal (31), in agreement with the findings in Refs. 4, 6, 14, 23. Thus, although most of the presented results were obtained for $\nu = 0.40$ and $\rho_p/\rho_s = 1.60$, they are valid for $0.25 \leq \nu \leq 0.48$ and $1.40 \leq \rho_p/\rho_s \leq 2.50$, with sufficient accuracy for most applications.

Table 1 lists the twenty-five combinations of moduli ratio, E_p/E_s, and slenderness ratio, L/d, studied in this paper. Results are presented only for an average hysteretic damping ratio $\beta = 0.05$, although several analyses with $\beta = 0.02$ have also been performed in the course of this work (31). For each of the twenty-five combinations the frequency factor, a_s, varies from 0.01 to 1.2. Thus, the presented information encompasses a very wide range of parameters, covering most practical situations.

Static Stiffnesses

By allowing the frequency of oscillation to approach zero one can study the static behavior of laterally loaded constrained-head piles—a problem for which only a limited number of approximate continuum-type solutions has so far been published (2,21), in addition, of course, to Winkler

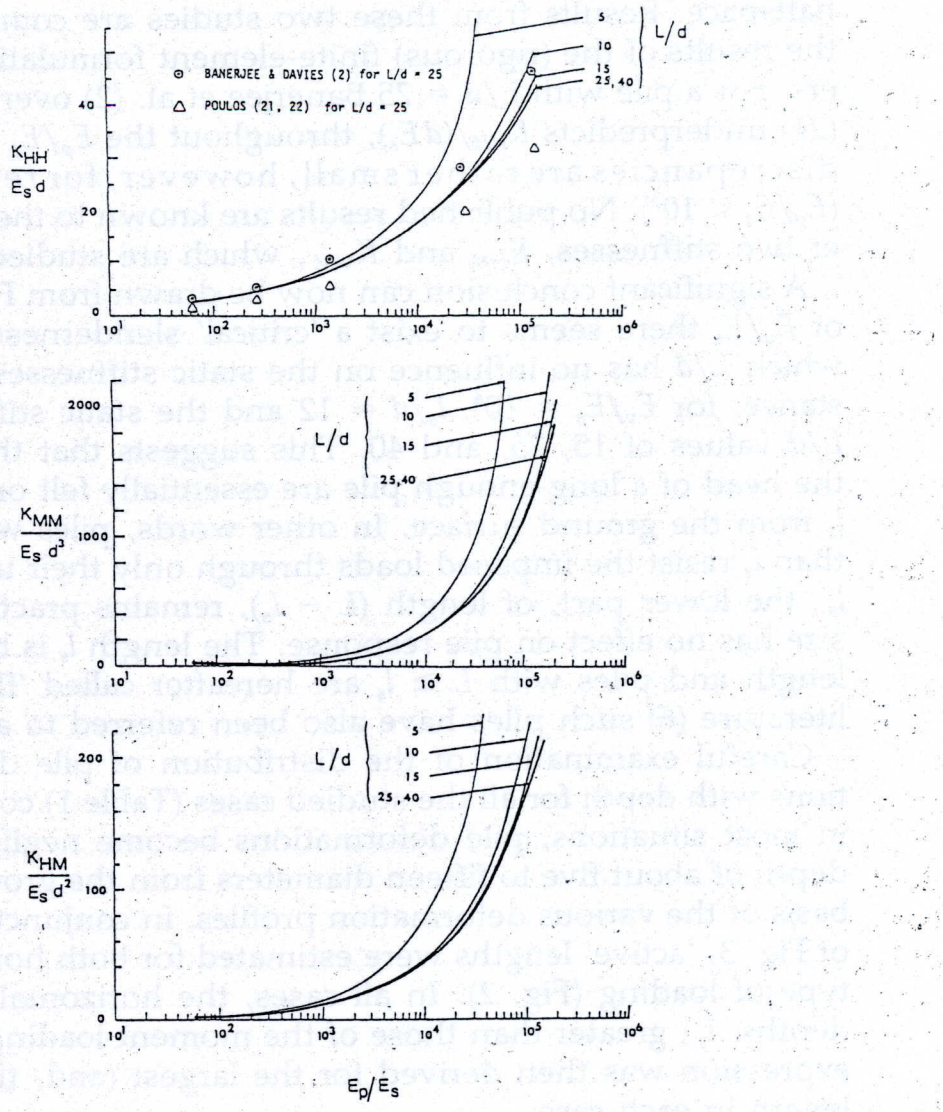

FIG. 3.—Dependence on Static Stiffnesses on E_p/E_s and L/d

foundation-type solutions with subgrade modulus proportional to depth (16,28).

Figure 3 portrays the dependence of the three normalized static stiffnesses, $K_{HH}/(dE_s)$, $K_{MM}/(d^3E_s)$ and $K_{HM}/(d^2E_s)$, on the two most crucial parameters of the system, E_p/E_s and L_d. It is noticed that, with the exception of very short and rigid piles ($L/d \leq 5$, $E_p/E_s \geq 10^4$), static pile stiffnesses are quite insensitive to variations in L/d, but tend to increase substantially with increasing E_p/E_s. Especially sensitive to increases in E_p/E_s is the rocking stiffness.

Poulos (21,22) and Banerjee and Davies (2) have presented results for the static horizontal displacement of fixed-head piles embedded in soil with modulus proportional to depth. Their solutions, however, are only approximate: Poulos (21) utilized Mindlin's expressions for a homogeneous soil by making the simplifying assumption that a point load induces on two identical points in a nonhomogeneous and a homogeneous halfspace displacements which are inversely proportional to the respective moduli at these points; Banerjee and Davies (2) extended Mindlin's solution to a point load acting at the interface of a two-layer halfspace and then empirically extrapolated it to a linearly nonhomogeneous

halfspace. Results from these two studies are compared in Fig. 3 with the results of the (rigorous) finite-element formulation used by the writers. For a pile with $L/d = 25$ Banerjee et al. (2) overpredict while Poulos (21) underpredicts $K_{HH}/(dE_s)$, throughout the E_p/E_s range examined; the discrepancies are rather small, however, for relatively 'soft' piles ($E_p/E_s < 10^3$). No published results are known to the authors for the other two stiffnesses, K_{HM} and K_{MM}, which are studied herein.

A significant conclusion can now be drawn from Fig. 3. For each value of E_p/E_s there seems to exist a 'critical' slenderness ratio, l_s/d, beyond which L/d has no influence on the static stiffnesses of the pile. For instance, for $E_p/E_s = 10^4$, $l_s/d \approx 12$ and the static stiffnesses coincide for L/d values of 15, 25, and 40. This suggests that the loads imposed at the head of a long-enough pile are essentially felt only down to a depth l_s from the ground surface. In other words, piles with length L greater than l_s resist the imposed loads through only their upper part, of length l_s; the lower part, of length $(L - l_s)$, remains practically "idle" and its size has no effect on pile response. The length l_s is being named 'active' length and piles with $L \geq l_s$ are hereafter called 'flexible' piles. In the literature (6) such piles have also been referred to as 'long' piles.

Careful examination of the distribution of pile deflections and rotations with depth for all the studied cases (Table 1) confirms that, indeed, in most situations, pile deformations become negligibly small below a depth of about five to fifteen diameters from the ground surface. On the basis of the various deformation profiles, in conjunction with the results of Fig. 3, 'active' lengths were estimated for both horizontal and rocking type of loading (Fig. 2). In all cases, the horizontal loading influenced depths, l_s, greater than those of the moment loading. A unique, simple expression was then derived for the largest (and, thus, critical) 'active' length in each case:

$$\frac{l_s}{d} \simeq 1.75 \left(\frac{E_p}{E_s}\right)^{0.21} \quad \ldots\ldots (6)$$

The accuracy of Eq. 6 (error within 10%) is sufficient for most applications. At depths below $z = l_s$ a statically loaded pile will sustain deformations less than 5% of the corresponding head deformations; furthermore, removing the lower (non-active) portion of a pile will affect by less than 0.1% its head static stiffnesses.

For 'flexible' piles, i.e., piles with $L \geq l_s$, the slenderness ratio, L/d, has no effect on the response, which may, thus, be uniquely related to E_p/E_s. The following simple algebraic formulas fit the length-independent curves of Fig. 3 with a very reasonable accuracy and are, hence, recommended for practical use:

$$\frac{K_{HH}}{dE_s} \simeq 0.60 \left(\frac{E_p}{E_s}\right)^{0.35} \quad \ldots\ldots (7a)$$

$$\frac{K_{MM}}{d^3E_s} \simeq 0.14 \left(\frac{E_p}{E_s}\right)^{0.80} \quad \ldots\ldots (7b)$$

$$\frac{K_{HM}}{d^2E_s} \simeq -0.17 \left(\frac{E_p}{E_s}\right)^{0.60} \quad \ldots\ldots (7c)$$

Swaying.—Figures 4 and 5 portray the dependence of $K_{HH}/(dE_s)$ and D_{HH}, respectively, on the frequency factor, $a_s = \omega d/V_s$, the moduli ratio, E_p/E_s, and the slenderness ratio, L/d, for an average hysteretic damping ratio in the soil $\beta = 0.05$. The practical usefulness of these plots arises from their nondimensional form and the wide range of system parameters considered.

Several features regarding the dynamic stiffness are worthy of note in Fig. 4.

In general, K_{HH} exhibits only a small sensitivity to variations in frequency. For slender piles and relatively stiff soil, in particular, use of a frequency-independent stiffness seems to be accurate enough in most applications; the static stiffness computed from Eq. 7*a* can then be used approximately at any frequency of oscillation. On the other hand, for very stiff and short piles (e.g., with $E_p/E_s \geq 29{,}000$ and $L/d \leq 10$) oscillating at high frequency factors, K_{HH} attains appreciable smaller than its static low-frequency values.

Moreover, resonance phenomena create a valley in all the stiffness-vs.-frequency curves. The sharpness of the valley increases with decreasing L/d, while the frequency of the minimum value essentially coincides with the fundamental natural frequency of the soil deposit, ω_1, in vertically propagating shear waves. Indeed, ω_1 of a soil deposit with modulus proportional to depth is given by (e.g., 5)

$$\omega_1 \simeq 1.20 \frac{V_s}{L} \left(\frac{L}{d}\right)^{1/2} \quad \text{(8)}$$

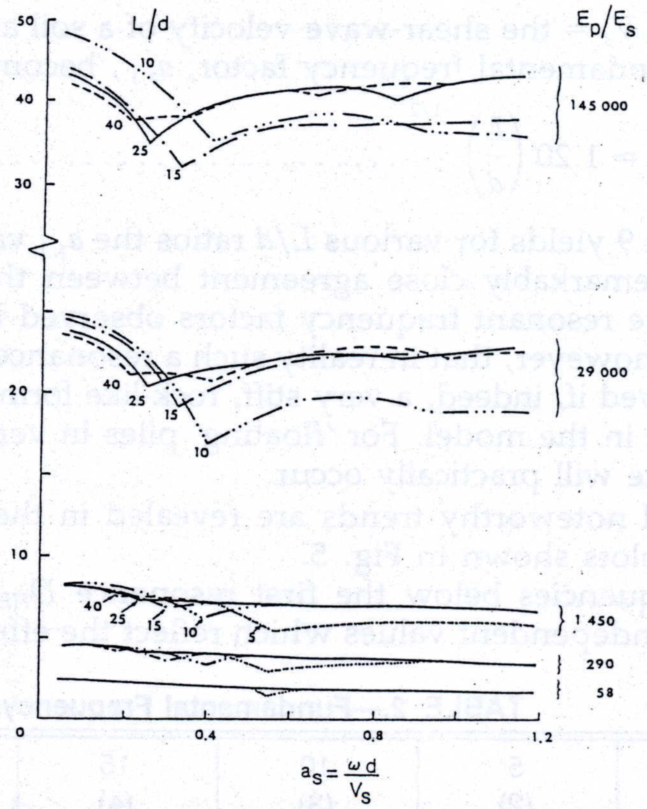

FIG. 4.—Variation of Dynamic Swaying Stiffness with a_s, E_p/E_s and L/d ($\beta = 0.50$)

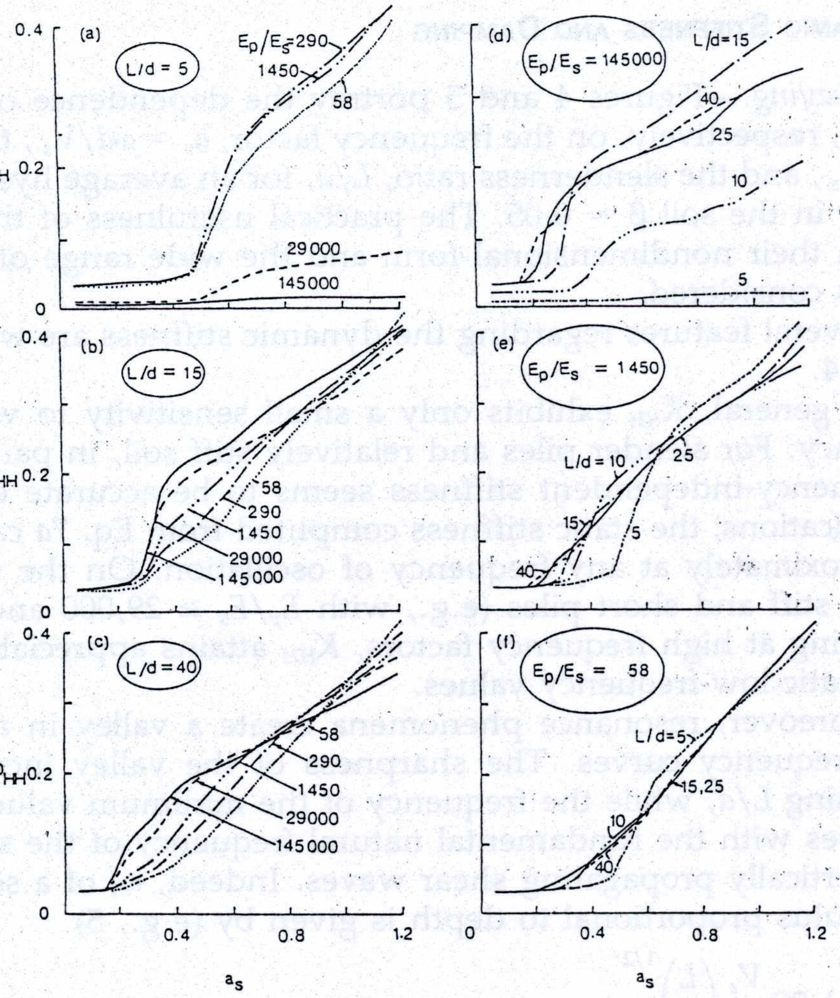

FIG. 5.—Variation of Swaying Damping Ratio with a_s, E_p/E_s and L/d (β = 0.50)

in which V_s = the shear-wave velocity of a soil at depth $z = d$. From Eq. 8, the fundamental frequency factor, $a_{s,1}$, becomes

$$a_{s,1} = \frac{\omega_1 d}{V_s} \simeq 1.20 \left(\frac{L}{d}\right)^{-1/2} \quad \text{.......} \quad (9)$$

Equation 9 yields for various L/d ratios the $a_{s,1}$ values displayed in Table 2. The remarkably close agreement between these $a_{s,1}$ values and the respective resonant frequency factors observed in Fig. 5 are apparent.

Note, however, that in reality such a resonance phenomenon will only be observed if, indeed, a very stiff, rock-like formation exists at the depth assumed in the model. For 'floating' piles in very deep soil deposits no resonance will practically occur.

Several noteworthy trends are revealed in the damping ratio-vs.-frequency plots shown in Fig. 5.

At frequencies below the first resonance D_{HH} attains small and frequency-independent values which reflect the effective material damping

TABLE 2.—Fundamental Frequency Factors

L/d (1)	5 (2)	10 (3)	15 (4)	25 (5)	40 (6)
$a_{s,1}$	0.54	0.38	0.31	0.24	0.19

in the system (of a hysteretic nature). No radiation damping is present since neither surface nor body radially-propagating waves can be physically sustained in the soil stratum at such low frequencies. Above the fundamental frequency of the stratum, ω_1, D_{HH} increases monotonously with a_s—an indirect evidence of the developing radiation damping.

The low-frequency values of the effective (hysteretic) damping ratio range from 0.002, for the most rigid and shortest of the examined piles (E_p/E_s = 145,000, L/d = 5), to 0.033, for all the (statically) 'flexible' piles ($L > l_s$). These D_{HH} values are, invariably, smaller than the average hysteretic damping ratio in the soil, β = 0.05. This is quite understandable since an important part of the system, the pile itself, has been considered as being of purely elastic material, with no damping at all.

The low-frequency damping ratio of a 'flexible' pile (i.e., with $L > l_s$) appears to be independent of both E_p/E_s and L/d. On the other hand, the more "rigidly" a pile behaves under lateral loads, the smaller is the (hysteretic) damping ratio of the system, at low frequencies. Thus, for example, keeping L/d constant equal to 5 while increasing E_p/E_s from 58 to 1,450 has no effect on the low-frequency D_{HH} (Fig. 5(*a*)); further increasing E_p/E_s to 29,000 and 145,000, however, leads to a dramatic decline in D_{HH}. A similar trend can be observed in Fig. 5(*d*) where E_p/E_s remains constant, 145,000, while L/d decreases from 40 to 5.

Beyond the "cut-off" frequency factor, $a_{s,1}$ (Eq. 9), the D_{HH} vs. a_s relationship seems to be dependent on the nature of pile behavior ('flexible' or 'non-flexible') and on E_p/E_s. As seen mainly in Figs. 5(*a*) and 5(*d*), even at high frequencies 'flexible' piles attain D_{HH} values larger than those experienced by 'rigid and short' piles. Moreover, it is interesting to notice (Figs. 5(*d*), 5(*e*), and 5(*f*)) that, for 'flexible' piles, high-frequency D_{HH} is independent of L/d but fairly sensitive to E_p/E_s; when E_p/E_s increases, the slope of the $D_{HH}(a_s)$ curve becomes less steep, which indicates that the relative contribution of radiation damping tends to decline.

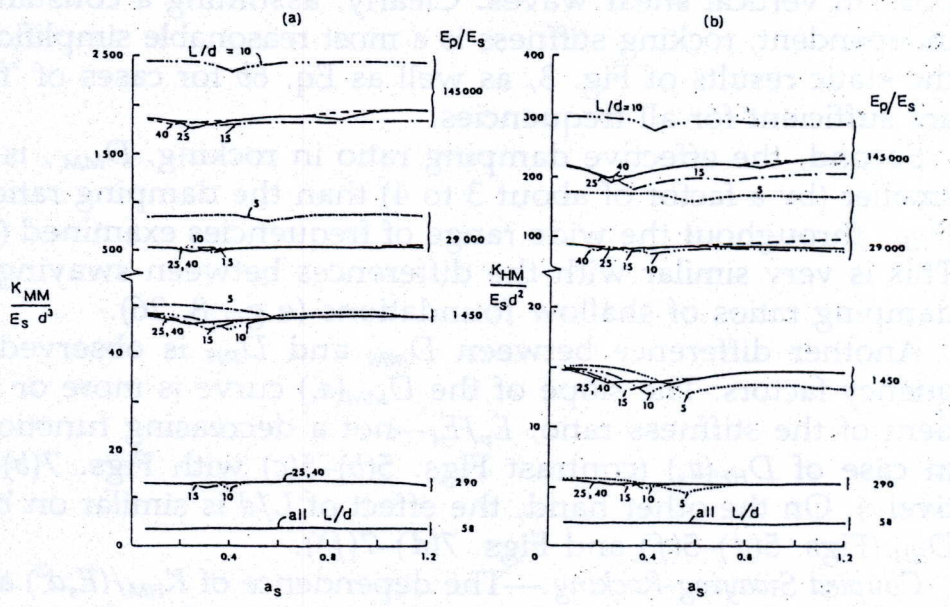

FIG. 6.—(*a*) Variation of Dynamic Rocking Stiffness with a_s, E_p/E_s and L/d (β = 0.05); (*b*) Variation of Coupled Swaying-Rocking Dynamic Stiffness with a_s, E_p/E_s and L/d (β = 0.05)

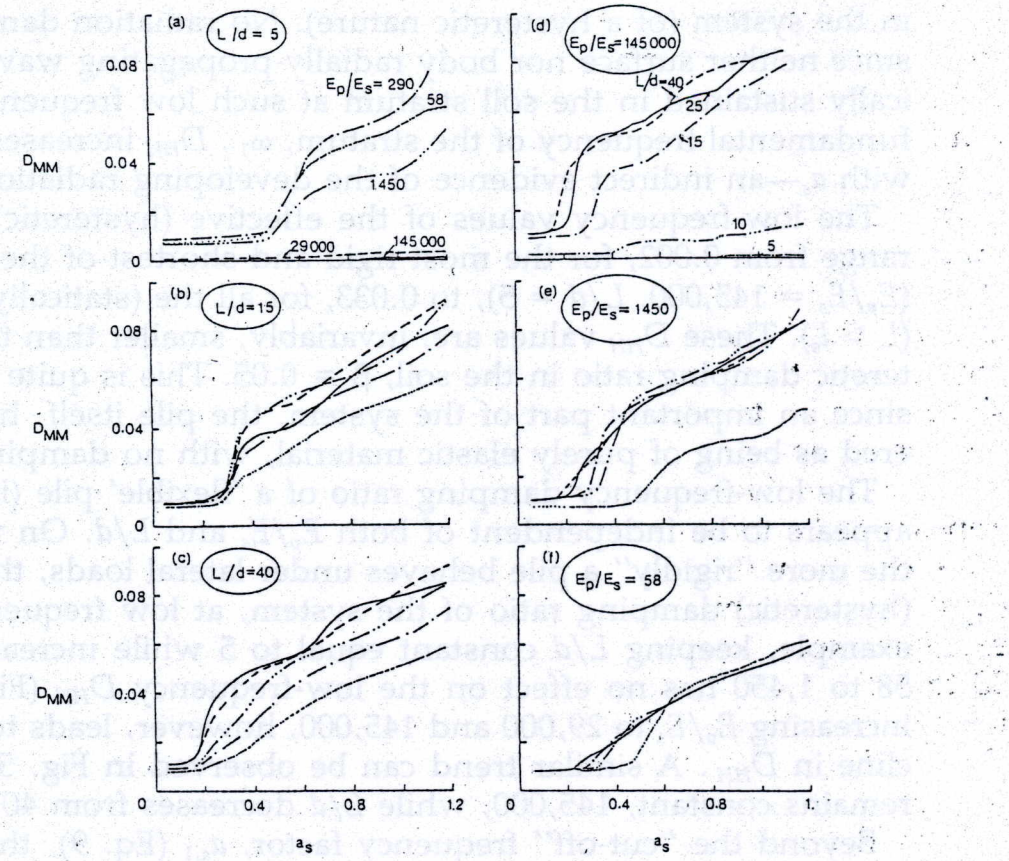

FIG. 7.—Variation of Rocking Damping Ratio with a_s, E_p/E_s and L/d ($\beta = 0.50$)

Rocking.—The dependence of $K_{MM}/(E_s d^3)$ and D_{MM} upon a_s, E_p/E_s and L/d is portrayed in Fig. 6(*a*) and Fig. 7, respectively, for an average hysteretic damping ratio in the soil $\beta = 0.05$. The main differences between swaying and rocking are summarized below.

First, rocking stiffness is very insensitive to variations in frequency, exhibiting a very flat resonant valley at the natural frequency of the deposit in vertical shear waves. Clearly, assuming a constant, frequency-independent, rocking stiffness is a most reasonable simplification. Hence, the static results of Fig. 3, as well as Eq. 6*b* for cases of 'flexible' piles, are sufficient for all frequencies.

Second, the effective damping ratio in rocking, D_{MM}, is substantially smaller (by a factor of about 3 to 4) than the damping ratio in swaying, D_{HH}, throughout the wide range of frequencies examined ($0 < a_s \leq 1.2$). This is very similar with the differences between swaying and rocking damping ratios of shallow foundations (e.g., 8, 26).

Another difference between D_{MM} and D_{HH} is observed at high frequency factors: The slope of the $D_{MM}(a_s)$ curve is more or less independent of the stiffness ratio, E_p/E_s—not a decreasing function of E_p/E_s as in case of $D_{HH}(a_s)$ (contrast Figs. 5(*b*)–5(*c*) with Figs. 7(*b*)–7(*c*), respectively). On the other hand, the effect of L/d is similar on both D_{MM} and D_{HH} (Figs. 5(*d*)–5(*f*) and Figs. 7(*d*)–7(*f*)).

Coupled Swaying-Rocking.—The dependence of $K_{HM}/(E_s d^2)$ and D_{HM} upon a_s, E_p/E_s and L/d is shown in Fig. 6(*b*) and Fig. 8, respectively. It is evident that the coupled swaying-rocking impedance combines the key features observed in swaying (Figs. 4 and 5) and rocking (Figs. 6(*a*) and 7); hence, no further discussion seems necessary herein.

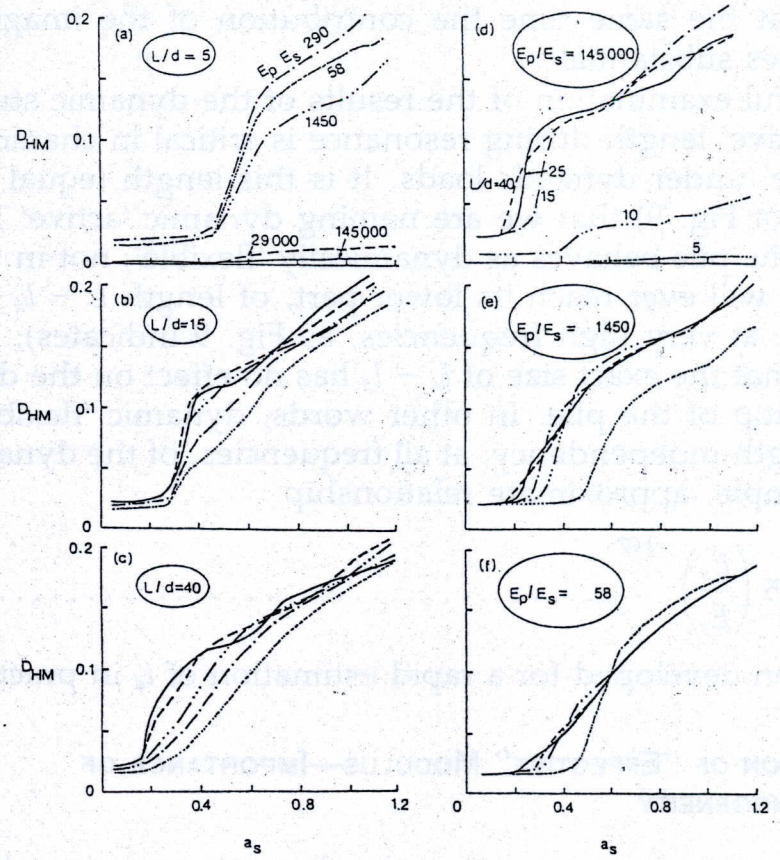

FIG. 8.—Variation of Coupled Swaying-Rocking Damping Ratio with a_s, E_p/E_s and L/d ($\beta = 0.50$)

'Active' Length Under Dynamic Loading.—With increasing frequency of oscillation, the 'active' length of a 'flexible' pile tends to increase beyond the static value computed from Eq. 6. As an example, Fig. 9 shows a typical set of distributions of dynamic deflections with depth, for a horizontally loaded fixed-head pile of $E_p/E_s = 29{,}000$ and $L/d = 25$. Three excitation frequency factors are studied: $a_s = 0.056$, corresponding to near-static conditions; $a_s = 0.240$, corresponding to the resonant frequency of the system (Table 2); and $a_s = 0.842$, corresponding to high frequencies. At the lowest frequency, the 'active' length is about $15d$, essentially equal to the static 'active' length, l_s (Eq. 6). By the time resonance is reached, the 'active' length has increased to about $20d$, with no significant change in the deflected shape of the pile. Finally, beyond resonance, the shape of the deforming pile undergoes changes, exhibiting a "wavy" character,

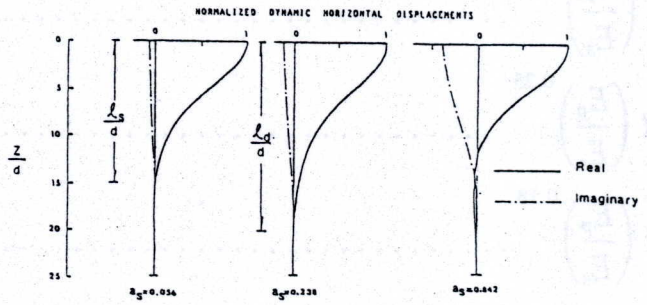

FIG. 9.—Typical Profiles of Dynamic Horizontal Displacement of Fixed-Head Flexible Piles; Definition of l_d

while at the same time the contribution of the imaginary component increases substantially.

Careful examination of the results of the dynamic study revealed that the 'active' length during resonance is critical in characterizing a pile as 'flexible' under dynamic loads. It is this length (equal to 20d in the example of Fig. 9) that we are naming dynamic 'active' length, l_d. When $L \geq l_d$ the pile behaves as dynamically 'flexible'; not in the sense that no motion will ever reach its lower part, of length $L - l_d$ (this is certain to happen at very high frequencies, as Fig. 9 indicates); but rather in the sense that the exact size of $L - l_d$ has no effect on the dynamic response at the top of the pile. In other words, dynamic 'flexibility' stems from the length-independency, at all frequencies, of the dynamic impedances. The simple, approximate relationship

$$\frac{l_d}{l_s} \simeq 2.75 \left(\frac{E_p}{E_s}\right)^{-0.07} \quad \text{(10)}$$

has been developed for a rapid estimation of l_d in practical applications.

Selection of "Effective" Modulus—Importance of Nonhomogeneity

It is instructive to compare the dynamic response characteristics of a pile embedded in a nonhomogeneous and then in an appropriately selected homogeneous deposit. To this end, it is convenient to first define a statically "equivalent" homogeneous stratum, which, in any particular mode, leads to a static pile stiffness identical with the stiffness of the same pile in the actual nonhomogeneous deposit. The modulus of such an "equivalent" stratum is herein named "effective" modulus, $\bar{E}$. This modulus corresponds to an "effective" point at a depth $\bar{z}$ below the ground surface of the actual deposit.

It has been found that, for a given nonhomogeneous stratum, the depth $\bar{z}$ of the effective point depends not only on pile geometry and stiffness, but also on the type of loading considered. Thus, there exist three different depths, $\bar{z}_{HH}$, $\bar{z}_{MM}$ and $\bar{z}_{HM}$, for each of the three modes studied in the paper (Fig. 2). Algebraic formulas appropriate for 'flexible' piles have been derived for these three variables, by comparing Eqs. 7 with the pertinent expressions given for homogeneous deposits in Refs. 6 and 4. With reasonable accuracy

$$\bar{z}_{HH} \simeq 0.50d \left(\frac{E_p}{E_s}\right)^{0.19} \quad \text{(11a)}$$

$$\bar{z}_{MM} \simeq 0.45d \left(\frac{E_p}{E_s}\right)^{0.25} \quad \text{(11b)}$$

$$\bar{z}_{HM} \simeq 0.80d \left(\frac{E_p}{E_s}\right)^{0.18} \quad \text{(11c)}$$

Equations 11, plotted in Fig. 10, reveal that, in most situations, the "effective" points lie only about 2 to 4 diameters beneath the surface. Two other features are worthy of note. First, the "effective" depth, $\bar{z}_{MM}$, for

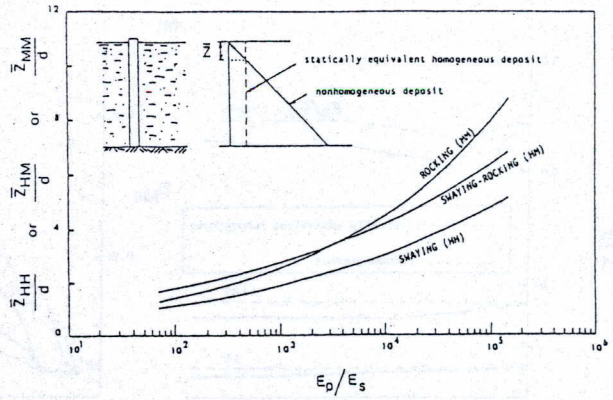

FIG. 10.—Dependence of Depths of Three "Effective" Points on the Moduli Ratio

rocking is always larger than the "effective" depth, $\bar{z}_{HH}$, for swaying. This is quite understandable in view of the restrained deflections immediately below the head of a pile in rocking (Fig. 2*b*)); in contrast, the largest deflections of a pile in swaying occur at the ground surface (Fig. 2(*a*)). Furthermore, increasing the relative stiffness, E_p/E_s, of a pile tends to move the "effective" points deeper, regardless of loading conditions. This, again, is hardly surprising: enhancing the flexural rigidity of a pile increases the deformations experienced at larger depths while reducing their concentration near the surface. One may readily verify the above statement by observing the increase in l_s (Eq. 6).

A convenient way of describing the dynamic effects of soil nonhomogeneity on pile stiffnesses is to observe the error involved in replacing the actual soil deposit by a statically "equivalent" homogeneous one. To this end, Fig. 11 studies the variation with a_s of the swaying and rocking impedances of three flexible piles embedded first in a linearly nonhomogeneous and then in the respective statically "equivalent" deposits. All three piles have an L/d ratio of 25, but three different E_p/E_s ratios, 58, 1,450 and 29,000.

It is evident from Fig. 11 that static "equivalence" does not guarantee identical pile response under dynamic loads. The discrepancies between the two sets of solutions range from negligibly small, in the rocking stiffnesses of all three piles; to appreciable, in the swaying stiffnesses of the relatively rigid piles; and to substantial, in the effective damping ratio of all piles in both modes. The following trends are worthy of some discussion:

1. Resonant frequencies are underpredicted (by a factor of about 2) when using the "equivalent" homogeneous solutions. The explanation is straightforward: with all three piles, the location of the "effective point, controlled solely by static deformations, is only about 1 to 4 diameters below the surface (Fig. 11); whereas, during resonance, up and down propagating waves affect the soil at greater depths and, hence, the "effective" point for computing the fundamental frequency is located near the middle of the deposit (5). As the soil modulus at this latter depth, $L/2$ (= $12.5d$), is higher than the "effective" modulus, $\bar{E}$, at a depth of 1 to 4 diameters, the actual resonant frequencies are higher than the ones predicted with the "equivalent" homogeneous stratum. Note, of

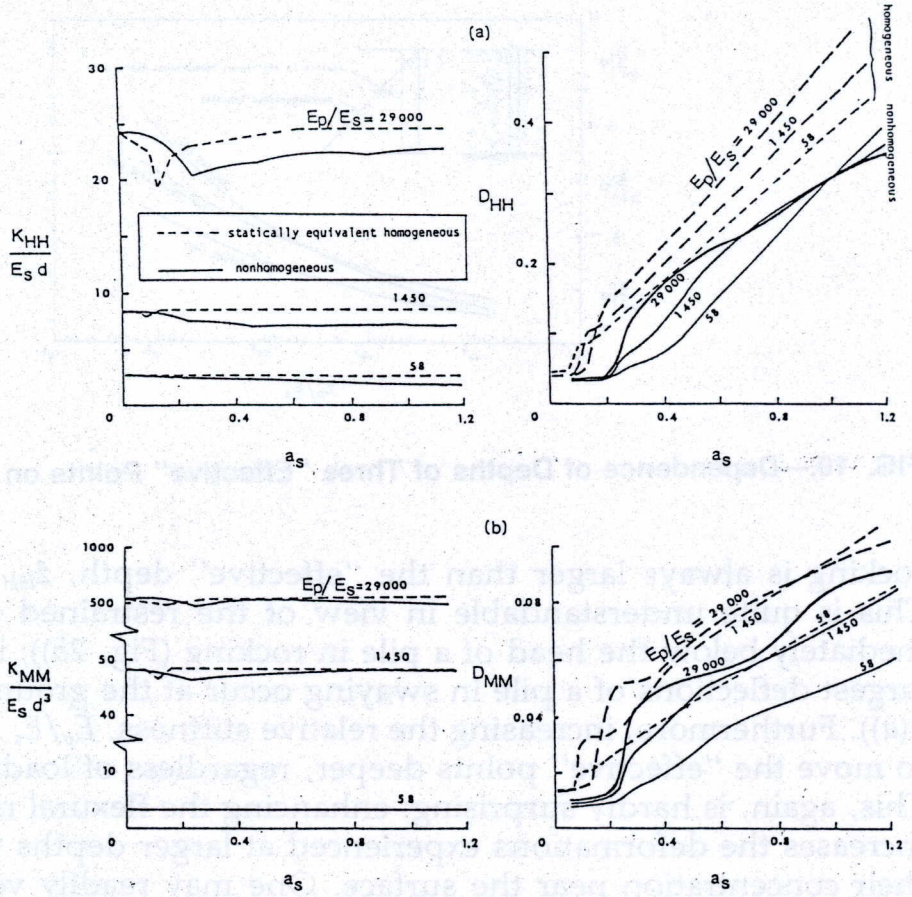

FIG. 11.—Comparison of Dynamic Stiffness and Damping of Three Flexible Piles Embedded in Nonhomogeneous and in Statically Equivalent Homogeneous Deposits: (*a*) Swaying; (*b*) Rocking

course, that this difference is of no importance in case of floating piles in very deep soil deposits.

2. At high frequency factors, the swaying stiffnesses of piles have smaller values in a non-homogeneous than in a statically "equivalent" homogeneous deposit.

3. Effective damping ratios are seriously overpredicted by the "equivalent" homogeneous solutions. This is true for both the hysteretic (frequency-independent) component and the radiation (increasing-with-frequency) component of damping. Furthermore, at high frequency factors, the actual $D_{HH}(a_s)$ curves tend to become less steep as E_p/E_s increases—exactly the opposite of what homogeneous solutions predict. A thorough explanation of all these differences seems a formidable task, which goes beyond the scope (and limited size) of this paper. For the time being, it is sufficient to caution that the larger than actual amount of damping, along with larger swaying stiffness, predicted at high frequencies by statically "equivalent" homogeneous deposits may often lead to unsafe designs of pile foundations.

Summary and Conclusions

Results of a finite-element-based comprehensive parameter study are presented for the static and dynamic stiffnesses and the effective damping ratios at the head of laterally loaded piles embedded in a soil stratum

with modulus proportional to depth. With these results one can obtain estimates of the dynamic response of foundations and structures supported by piles, using the standard procedures developed for shallow foundations (8,26).

The results presented herein are strictly applicable only to 'end-bearing' piles. In case of 'floating' piles in deep soil deposits, the results are still valid as long as the pile is 'flexible' ($L > l_s$ or l_d). For "short and rigid" piles, however, the assumed model can hardly reproduce practical situations, as it requires the presence of a rigid stratum at relatively shallow depths, which may rather infrequently occur in nature.

The stiffness ratio, E_p/E_s, where E_s is the soil Young's modulus at a one-diameter depth, has been found to be the most crucial dimensionless parameter of the system; the slenderness ratio, L/d, is of importance only in cases of very rigid and short piles. Moreover, the dimensionless factor, a_s, associated with the frequency of excitation, influences strongly the effective damping ratios and, to a lesser extent, the dynamic swaying stiffness of a pile. Non-dimensional graphs display the effects of these parameters for swaying, rocking and coupled swaying-rocking modes of excitation; these results encompass the wide range of problem parameters expected in practical situations.

The presented graphs and formulas are particularly suited for preliminary design calculations of pile foundations. However, care and engineering judgement must be exercised before applying these results in actual situations. Several phenomena which may appreciably affect pile behavior in certain cases have been either ignored or only approximately modeled in the formulation. For instance, nonlinear hysteretic soil behavior has only indirectly been reflected in the analysis, through the selection of a soil stratum with a linearly increasing modulus and a linearly decreasing hysteretic damping ratio with depth. Perfect contact has been assumed at the pile-soil interface, while, in reality, separation and gapping may reduce both stiffness and radiation damping under a strong excitation. Finally, no consideration has been given to the potentially significant effects of the interaction with neighboring piles. Nonetheless, it is clear that important trends and conclusions reached in this study have offered a valuable insight to the mechanics of the problem and can serve as a useful guide in analysis and design of laterally loaded piles.

APPENDIX.—REFERENCES

1. Angelides, D. C., and Roesset, J. M., "Non-Linear Lateral Dynamic Stiffness of Piles," *Journal of the Geotechnical Engineering Division*, ASCE, Vol. 107, No. GT11, 1981, pp. 1443–1460.
2. Banerjee, P. K., and Davies, T. G., "The Linear Behaviour of Axially and Laterally Loaded Single Piles Embedded in Nonhomogeneous Soils," *Geotechnique*, Vol. 28, No. 3, 1978, pp. 309–326.
3. Bea, R. G., "Dynamic Response of Piles in Offshore Platforms," *Dynamic Response of Pile Foundations: Analytical Aspects*, ASCE, 1980, pp. 80–105.
4. Blaney, G. W., Kausel, E., and Roesset, J. M., "Dynamic Stiffness of Piles," *Proceedings of the Second International Conference on Numerical Methods in Geomechanics*, ASCE, Blacksburg, Va., 1976, pp. 1001–1012.
5. Dobry, R., Oweis, I., and Urzua, A., "Simplified Procedures for Estimating the Fundamental Period of a Soil Profile," *Bulletin of the Seismological Society of America*, Vol. 66, No. 4, Aug., 1976, pp. 2193–1321.

6. Dobry, R., Vicente, E., O'Rourke, M. J., and Roesset, J. M., "Horizontal Stiffness and Damping of Single Piles," *Journal of the Geotechnical Engineering Division*, ASCE, Vol. 108, No. GT3, 1982, pp. 439–459.
7. Gazetas, G., "Static and Dynamic Displacements of Foundations on Heterogeneous Multilayered Soils," *Geotechnique*, Vol. 30, No. 2, 1980, pp. 159–177.
8. Gazetas, G., "Analysis of Machine Foundation Vibrations: State of the Art," *International Journal of Soil Dynamics and Earthquake Engineering*, Vol. 2, No. 1, 1983, pp. 2–42.
9. Harada, T., Kubo, K., and Katayama, T., "Dynamic Soil-Structure Interaction by Continuum Formulation Method," *Report of the Institute of Industrial Science*, University of Tokyo, Vol. 29, No. 5, 1981, pp. 1–194.
10. Jamiolkowski, M., and Garassino, A., "Soil Modulus for Laterally Loaded Piles," *Proceedings of the Specialty Session No. 10*, 9th International Conference on Soil Mechanics and Foundation Engineering, Tokyo, 1977, pp. 43–58.
11. Kagawa, T., and Kraft, L. M., "Lateral Load-Deflection Relationship of Piles Subjected to Dynamic Loadings," *Soils and Foundations*, Vol. 20, No. 4, 1980, pp. 19–36.
12. Kagawa, T., and Kraft, L. M., "Dynamic Characteristics of Lateral Load-Deflection Relationships of Flexible Piles," *Earthquake Engineering and Structural Dynamics*, Vol. 9, 1981, pp. 53–68.
13. Kausel, E., Roesset, J. M., and Waas, G., "Dynamic Analysis of Footings on Layered Media," *Journal of the Engineering Mechanics Division*, ASCE, Vol. 101, No. EM5, 1975, pp. 679–693.
14. Kuhlemeyer, R. L., "Static and Dynamic Laterally Loaded Floating Piles," *Journal of the Geotechnical Engineering Division*, ASCE, Vol. 105, No. GT2, 1979, pp. 289–304.
15. Liou, D. D., and Penzien, J., "Seismic Analysis of an Offshore Structure Supported on Pile Foundations," *Report No. EERC77-25*, University of California, Berkeley, Calif., 1977.
16. Matlock, H., and Reese, L. C., "Generalized Solutions for Laterally Loaded Piles," *Journal of the Soil Mechanics and Foundations Division*, ASCE, Vol. 86, No. SM5, 1960, pp. 63–91.
17. Nogami, T., and Novak, M., "Resistance of Soil to a Horizontally Vibrating Pile," *International Journal of Earthquake Engineering and Structural Dynamics*, Vol. 5, 1977, pp. 239–262.
18. Novak, M., Nogami, T., and Aboul-Ella, F., "Dynamic Soil Reactions for Plane Strain Case," *Journal of the Engineering Mechanics Division*, ASCE, Vol. 104, No. EM4, 1978, pp. 953–959.
19. Novak, M., and Aboul-Ella, F., "Impedance Functions for Piles in Layered Media," *Journal of the Engineering Mechanics Division*, ASCE, Vol. 104, No. EM6, 1978, pp. 643–661.
20. Poulos, H. G., "Behaviour of Laterally Loaded Piles: I—Single Piles," *Journal of the Soil Mechanics and Foundations Division*, ASCE, Vol. 97, No. SM5, 1971, pp. 711–731.
21. Poulos, H. G., "Load-Deflection Prediction for Laterally Loaded Piles," *Australian Geomechanics Journal*, Vol. G3, No. 1, 1973, pp. 1–8.
22. Poulos, H. G., and Davis, E. H., *Pile Foundation Analysis and Design*, John Wiley and Sons, Inc., New York, N.Y., 1980.
23. Randolph, M. F., "Response of Flexible Piles to Lateral Loading, " *Geotechnique*, Vol. 31, No. 2, 1981, pp. 247–259.
24. Reese, L. C., Cox, W. R., and Koop, F. D., "Analysis of Laterally Loaded Piles in Sand," *Proceedings of the 6th Offshore Technology Conference*, Paper OTC 2080, Houston, Tex., 1974, pp. 473–483.
25. Reese, L. C., and Welch, R. C., "Lateral Loading of Deep Foundations in Stiff Clays," *Journal of the Geotechnical Engineering Division*, ASCE, Vol. 101, No. GT7, July, 1975, pp. 633–649.
26. Richart, F. E., Jr., Woods, R. D., and Hall, J. R., *Vibrations of Soils and Foundations*, Prentice-Hall, Inc., Englewood Cliffs, N.J., 1970.

27. Roesset, J. M., "Stiffness and Damping Coefficients of Foundations," *Dynamic Response of Pile Foundations: Analytical Aspects*, ASCE, 1980, pp. 1–30.
28. Scott, R. F., *Foundation Analysis*, Prentice-Hall, Inc., Englewood Cliffs, N.J., 1981.
29. Singh, A., Wei-Hu, R. E., and Cousineau, R. D., "Lateral Load Capacity of Piles in Sand and Normally Consolidated Clay," *Civil Engineering*, ASCE, Vol. 41, No. 8, 1971.
30. Tajimi, H., "Dynamic Analysis of a Structure Embedded in an Elastic Stratum," *Proceedings of the 4th World Conference on Earthquake Engineering*, Chile, 1969.
31. Velez, A. H., Gazetas, G., and Krishnan, R., "Lateral Stiffness and Damping of Constrained-Head Piles in Linearly Nonhomogeneous Soils," *Research Report CE82-06*, Rensselaer Polytechnic Institute, Troy, N.Y., 1982.